

Surface Topology Engineering of Membranes for the Mechanical Investigation of the Tubulin Homologue FtsZ**

Senthil Arumugam, Grzegorz Chwastek, Elisabeth Fischer-Friedrich, Carina Ehrig, Ingolf Mönch, and Petra Schwille*

In spite of their small size, bacteria display highly organized cytoskeletal structures like coils, helices, or rings. Extensive mechanical modeling has been done to explain the occurrence of such specific structures within the small volume of bacterial cells.^[1–4] As they are difficult to image within cells, in vitro reconstitution provides a valuable approach to quantitatively analyze their properties under defined conditions. A particularly interesting cytoskeletal feature is the Z-ring,^[5] which plays a key role in cell division for many bacteria. It is composed of FtsZ, a tubulin homologue, and other components and has been implicated in constriction force generation. Mechanisms localizing FtsZ to the center of the cell are known, but how it takes the form of a functional helical or ring-like structure remains unclear.^[5,6] We hypothesized that intrinsically curved FtsZ filaments should initially respond to the native shape of bacteria and align using geometric cues. Thus, we devised a controlled biomimetic platform with membrane-coated glass substrates mimicking biologically relevant curvatures, to elucidate the mechanical properties of membrane-associated FtsZ. We found that *E. coli* FtsZ is

assembled into inherently curved and twisted filaments supporting a helical geometry, which showed preferential orientations at the native bacterial cell-like curvatures. Strikingly, the FtsZ did not recognize smaller curvatures in the same way, but rather oriented themselves at an angle in higher curvatures, which does not support the idea that FtsZ alone is able to exert a constriction force.

In recent studies involving high-resolution imaging^[7] and cryo-electron microscopy,^[8] the “Z-ring” has generally been described as a helical structure. Purified FtsZ has been studied extensively by electron microscopy and atomic force microscopy.^[9–11] Consistently, the EM and AFM images from these studies show curved filaments.^[11–15] Cryo-EM on reconstituted FtsZ filaments in vitro seems to contradict the presence of any local spontaneous curvature.^[16] However, in a recent study, Osawa et al. showed the ability of FtsZ filaments with an artificially introduced membrane targeting sequence (MTS) to bend membranes, with an influence of the MTS placement in FtsZ on the membrane bending direction. They used an MTS from MinD at the C-terminus of FtsZ to mimic the recruitment of FtsZ to the membrane by adaptor proteins ZipA or FtsA. Upon shifting the MTS to the N-terminus, they find that the filaments bend the membrane in opposite directions. They interpret this to be caused by a constriction force produced by partial Z-rings.^[17]

A dividing bacterial cell initially has a curvature of about $2\ \mu\text{m}^{-1}$, but proceeds towards much higher curvature values as the cell progresses through division. It is unknown whether a bacterial membrane, fortified with many structural proteins, osmotic pressure, and a cell wall, would be as easily deformed. The spontaneous structure of FtsZ filaments may enable them to organize into highly curved suprastructures by sensing the inner cell-membrane curvature, but they may have to recruit other mechanically active factors for cytokinesis. The distortions observed in previous studies^[17,18] could simply be caused by a bundle of curved filaments bending the flexible membrane towards their own curvature.

We first repeated the experiments with MTS-FtsZ on free-standing giant unilamellar vesicle (GUV) membranes, and quantitatively evaluated the induced radii of curvature. We found that the filaments did not bend the membranes when the unilamellar vesicles were isotonic. They aligned into filament networks similar to those on planar supported bilayers (Figure 1b). Changing the osmotic gradient across the membranes by adding 10 mM glucose decreased intravesicular pressure and relaxed the membrane surface tension. This resulted in a curved topology of the membrane as well as the filaments (Figure 1a,b). Only when the membrane tension was low, under hypertonic conditions, could the filaments

[*] Prof. Dr. P. Schwille
Dept. Cellular and Molecular Biophysics, Max Planck Institute of Biochemistry

Am Klopferspitz 18, 82152 Martinsried (Germany)
E-mail: schwille@biochem.mpg.de


S. Arumugam, G. Chwastek, C. Ehrig^[†]
Max Planck Institute for Cell Biology and Genetics
Pfotenhauerstrasse 108, 01307 Dresden (Germany)
and
Biotechnology Center of the TU Dresden
Tatzberg 47/51, 01307 Dresden (Germany)

Dr. E. Fischer-Friedrich
Max Planck Institute for Physics of Complex Systems
Noethnitzerstrasse 38, 01187 Dresden (Germany)

Dr. I. Mönch
Leibniz Institute for Solid State and Materials Research
Helmholtzstraße 20, 01069 Dresden (Germany)

[†] Current address: Siemens AG, CT T DE HW3
Günther-Scharowsky-Str.1, 91058 Erlangen (Germany)

[**] We would like to thank Harold Erickson for the plasmids, Thomas Kurth for help with SEM, David Drechsel for help with protein purification, and German Rivas, Zdenek Petrask, and Benjamin Friedrich for discussions and suggestions. S.A. is supported by a PhD fellowship from Dresden International Graduate School for Biomedicine and Bioengineering. P.S. acknowledges the HFSP grant “Synthetic Biology of cell division: reconstructing the bacterial division machinery in the test tube”.

 Supporting information for this article (experimental details) is available on the WWW under <http://dx.doi.org/10.1002/anie.201204332>.

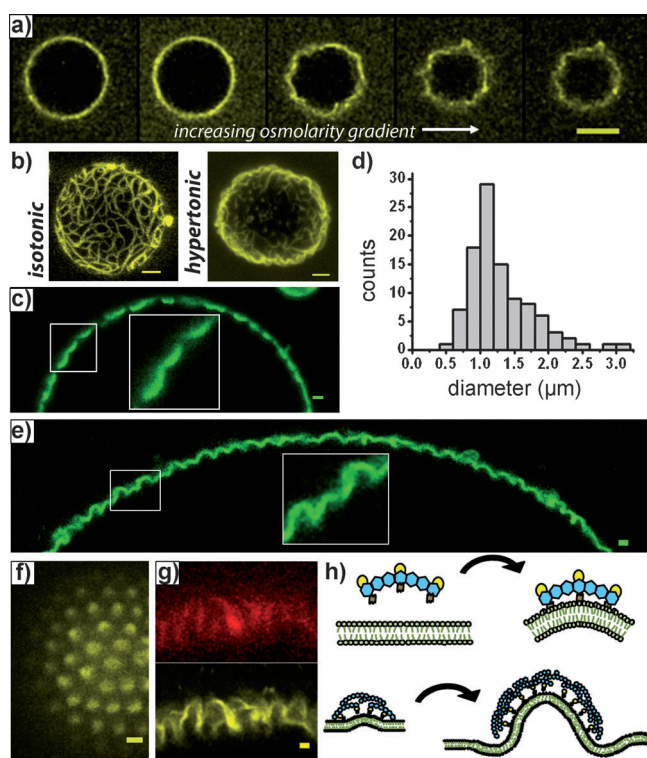


Figure 1. Assembly of FtsZ on GUVs. a) Fluorescence microscopy of a vesicle deflating with increasing osmolarity difference. b) FtsZ assembled on a vesicle in isotonic condition shows networks similar to planar supported bilayers, whereas in hypertonic conditions, vesicle shows curved filaments. c) FtsZ-YFP-MTS assembled on a GUV. d) Histogram of the radii of curvature from assembling the FtsZ-YFP-MTS on GUVs. e) MTS-FtsZ-YFP assembled on a GUV. f) Patches of MTS-FtsZ-YFP on the pole of the GUVs. g) Deformed membrane (top) and MTS-FtsZ-YFP (bottom). h) Scheme of the process of deformation of the membrane by FtsZ filaments. Scale bars: a) 10 μm ; b) 5 μm ; c–g) 1 μm .

imprint their spontaneous curvature on the membrane. Figure 1c and e show equatorial cross sections of GUVs with FtsZ-YFP-MTS and MTS-FtsZ-YFP (YFP = yellow fluorescent protein) producing spherical protrusions inwards and outwards, respectively. The mean diameter of the vesicles was about 1–1.25 μm (Figure 1d). We reasoned that spontaneously curved filaments should align on similarly curved supported membranes. The behavior of filaments with various curvature values should provide insight about the intrinsic structure of the FtsZ filaments.

To test the hypothesis that FtsZ protofilaments have spontaneous curvature, we assembled the filaments on bilayers formed on curved substrates. The curved substrates were produced using e-beam lithography; their profile was checked using AFM. Curvatures on grooved substrates were obtained using a novel oblique incidence angle e-beam etching technique (Supporting Information, Figures S1 and S2). A pre-curved filament should align along the direction of curvature, such that the bending energy of the polymer is minimized. Figure 2a,b shows the differential alignment of co-polymerized FtsZ and FtsZ-YFP-MTS filaments between planar crests and curved troughs by fluorescence imaging and

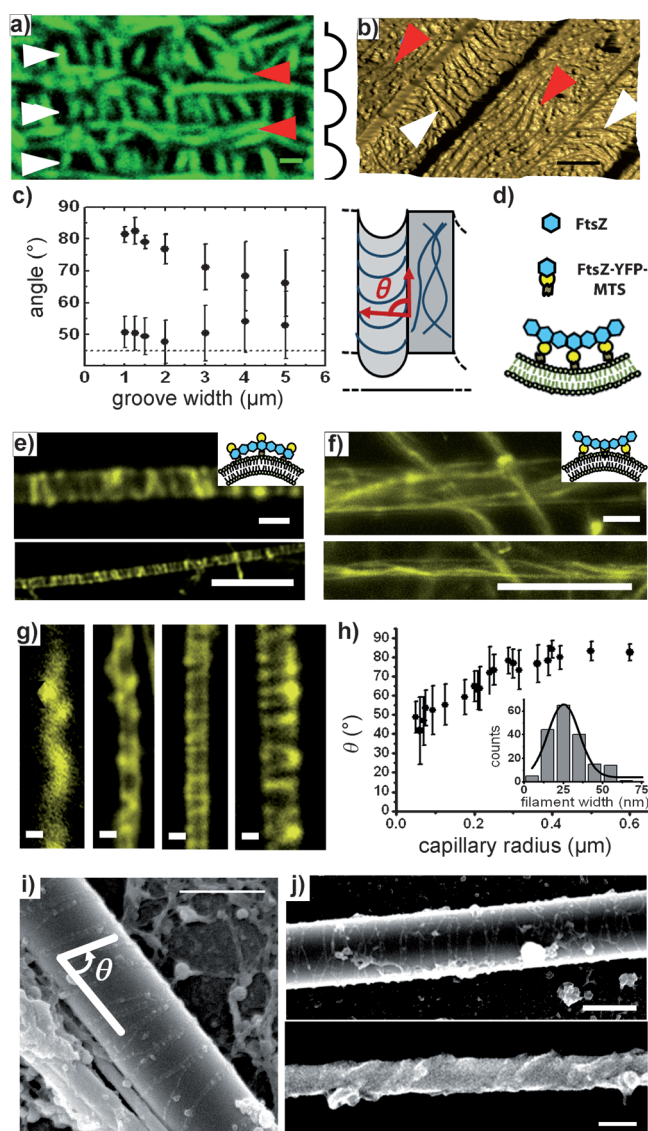


Figure 2. Interaction of FtsZ with curved membranes. a) FtsZ-YFP-MTS assembly on a membrane supported by a substrate with curved troughs (white arrows) and planar crests (red arrows). b) AFM image of the filaments assembled on the same substrate as in (a). c) Observed angles θ for FtsZ-YFP-MTS assembled on grooved supports with different radii of curvature. The scheme shows the measured filament orientation angle. Measurements on curved grooves (black) and control measurements on a planar area of similar geometry as used for the curved grooves (gray). d) Scheme of the FtsZ-YFP-MTS with spontaneous curvature binding to the membrane. e) MTS-FtsZ-YFP on glass capillaries. f) FtsZ-YFP-MTS on glass capillaries. Insets (e,f): schemes showing filament curvature with respect to the membrane curvature. g) MTS-FtsZ-YFP on glass capillaries of increasing sizes. h) Alignment of filaments with respect to the long axis of the capillary versus the radii of the capillaries. Inset: distribution of widths of measured filaments. i) SEM image of filaments on a capillary showing the measured angle θ . j) Filament arrangement on capillaries of diameter 500 nm (top) and 100 nm (bottom). Scale bars: a,b) 1.5 μm ; e,f) 1 μm (top), 10 μm (bottom); g,i) 1 μm ; j) 500 nm (top), 100 nm (bottom).

atomic force microscopy. Figure 2d is a schematic representation of FtsZ and FtsZ-YFP-MTS in polymerized form with an intrinsic curvature matching the membrane curvature.

To test the precision of alignment at different radii of curvatures, we measured the angle formed by the filament with respect to the long axis of the grooves (Figure 2c, Figure S3). We found that the near perpendicular alignment was most predominant at a radius of 1.25 μm . Experiments above these curvatures (grooves with smaller radii) were not feasible, owing to optical resolution limits and the inability of the AFM tips to scan the troughs. To probe the behavior of FtsZ filaments on curvatures higher than 1 μm^{-1} , we used positive curvature, achieved by coating glass capillaries with bilayers.

The glass capillaries were extracted from Whatman glass microfiber filters (GF/A), cleaned in alcohol, sonicated, and dried on a coverglass. The capillary diameters ranged from 100 nm to 2000 nm. These glass capillaries were then incubated with a solution of small unilamellar vesicles (SUV) and CaCl_2 to coat them with a bilayer. We assembled MTS-FtsZ-YFP, a version of FtsZ with the MTS at the N-terminus, on the bilayer-coated glass capillaries. This construct has the MTS on the opposite face of FtsZ compared to the construct with the C-terminal MTS.^[17] Spontaneously curved FtsZ filaments that aligned on grooves through the C-terminal MTS, should bind and align on capillaries through the N-terminal MTS. Consistent with the direction of spontaneous curvature, MTS-FtsZ-YFP could also align on glass rods of different sizes coated by lipid bilayers (Figure 2g). Figure 2e,f shows the difference in the orientation of the polymers depending on whether MTS-FtsZ-YFP or FtsZ-YFP-MTS were used. The filaments show constant turnover, as is expected from an active filament, resembling the *in vivo* structure (Figure S4–S7).

In contrast to grooves, capillaries allow for longer filaments to completely encircle the capillary and assemble complete rings or helices. For capillary diameters of 0.5 to 1 μm , the MTS-FtsZ-YFP filaments align almost perpendicularly to the longitudinal axis of the glass rod ($75 \pm 16^\circ$). Occasionally, 2–4 complete turns around the capillary were also observed. The FtsZ-YFP-MTS filaments, on the contrary, bind along the longitudinal axis of the rod ($23 \pm 12^\circ$). If spontaneous curvature and flexural rigidity of the FtsZ polymer accounts for the FtsZ alignment, then the alignment should be close to 90 degrees, as long as the spontaneous curvature matches the capillary curvature. Further, by using smaller capillary sizes, it should be possible to test the assumed high curvature ($10 \mu\text{m}^{-1}$) of the FtsZ polymers. Owing to the optical resolution limit, it was not possible to estimate capillary sizes or filament orientations accurately for capillaries below one micron in diameter by fluorescence microscopy (Figure 2g). Therefore, we performed scanning electron microscopy (SEM) on these samples and quantified the behavior of the filaments on the capillaries (Figure 2i,j). Figure 2h shows a plot of θ , the angle of the filament with respect to the long axis of the capillary, for different capillary radii. The mean width of the filaments were about 25 nm, about 4–7 subunits thick laterally (Figure 2h, inset). Figure 2j shows the assembly of filaments on two different sized

capillaries of 500 nm (top) and 100 nm (bottom). A simple model of a filament of smaller curvature attaching to a capillary of higher curvature aligning at an angle so as to match the spontaneous curvature with the directional curvature did not fully reconcile with our experimental observations (Figure 4a). This was highlighted by the fact that the mean curvature of filaments did not stay constant for different capillary radii (Figure S14) but increased towards smaller radii. However, we need to take into account that FtsZ helices winding around a cylindrical capillary are not characterized only by their curvature but also a non-vanishing twist if their pitch is not zero (Supporting Information, Text T2).

To better investigate the spontaneous shape of the FtsZ helices independent of a confining geometry, we explored the morphology of the polymers on a planar bilayer, where they are not confined by any given curved geometry, and therefore, they should settle close to their spontaneous geometrical configuration. Since fluorescence microscopy cannot resolve these structures owing to a limit in optical resolution, we performed AFM on the assembly to probe for any specific structures. AFM revealed the presence of abundant helical structures along with some filaments (Figure 3a). The twisted

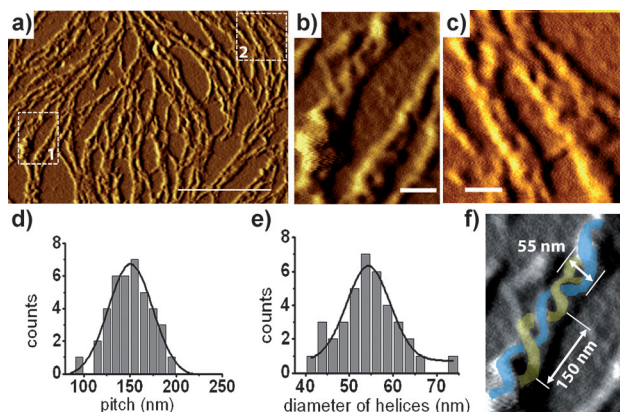


Figure 3. FtsZ polymers on planar bilayers. a) An AFM image of FtsZ filaments assembled on a planar supported *E. coli* lipid extract membrane. b,c) Zoomed image of boxed regions 1 and 2 from (a). d) Histogram of the pitch distribution. e) Histogram of the distribution of helix diameters. f) False colored helices with average values of pitch and diameter shown. Scale bar: a) 1 μm ; b,c) 100 nm.

filaments were woven into two filament helices as seen in the height image (Figure 3b,c). They show a pitch of about 150 nm and a diameter of about 55 nm (Figure 3d–f). These structures seem to confirm the presence of a finite twist along with a spontaneous curvature (Figure 4b). We assume that the helical structures assembled on bilayers represent the inherent structure of the FtsZ filaments. The values of the preferred curvature and the twist of the FtsZ helices on a capillary could then be approximated from the measured values of pitch and the diameters of the helices not confined by any curved geometry. We identified the curvature and the torsion of the helices measured on planar bilayers with the curvature and twist of FtsZ helices on the cylindrical capillaries (Supporting Information, Text T2).

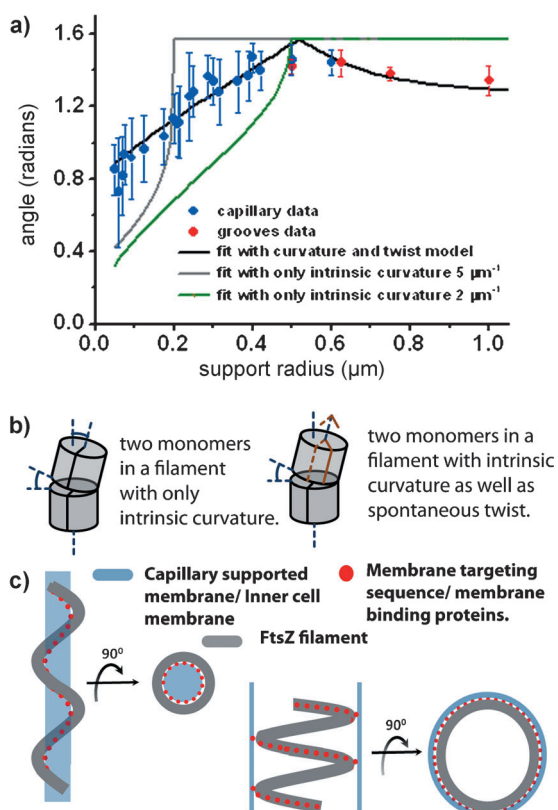


Figure 4. Curvature and twist in FtsZ filaments. a) Plot of angle versus curved support radius showing fits with different models (see legend). b) The difference between the two models from (a). c) Scheme showing filaments of MTS-FtsZ-YFP on capillaries with the MTS facing inwards or of FtsZ-YFP-MTS with the MTS facing outwards.

We modeled the behavior of helical filaments on a cylindrical surface, with the membrane targeting sequence facing inwards to the center of the cylinder, as in the case of MTS-FtsZ-YFP or outwards, as in the case of grooves with FtsZ-YFP-MTS (Figure 4c). The FtsZ filaments possess a helix and twist if the filaments are under no geometrical constraints. The conformational energy of the helix will be minimal at these values. In the presence of a geometrical confinement, as in the cases of a capillary or grooves, the filaments will take a conformation that minimizes the energy under the given geometrical constraints. The more the capillary diameter deviates from the native helix diameter (approximately 55 nm), the more the curvature and twist of the filament will deviate from its spontaneous values (Supporting Information, Text T2, Figure S14). Using the measured values of spontaneous curvature and twist, and energy minimization (Supporting Information, Text T2), we could fit the plot of angle versus radius (Figure 4a), in contrast to a model that only considered spontaneous curvature, which did not fit the data.

Many different shapes of non-membrane attached FtsZ filaments have been observed in various studies, mainly using EM and AFM.^[9,11,19–24] Almost all of these studies used electron microscopy grids, carbon grids, or mica supports to observe the filaments. The results also seem to depend on buffer conditions, sample preparation methods, and the

substrate used. Surface interactions may play a role in collapsing the filament away from its spontaneous structure. The filaments in the GTP-bound state should show turnover, an important property of the filaments observed in vivo. Our experiments were performed with filaments assembled on membranes that show normal turnover activity (Figures S4–S10). Moreover, the membrane allows the filament to slide and diffuse into the energy minimized state. We believe our in vitro system recapitulates the in vivo behavior of the essential FtsZ tethered to a curved membrane.

The behavior of filaments on capillaries of different radii agrees well with a model of intrinsic filament curvature and spontaneous twist, rather than a previously suggested model considering only spontaneous curvature.^[17,25] Therefore, our data strongly suggests that the *E. coli* FtsZ filaments have spontaneous curvature and twist. Photo-activated localization microscopy (PALM) studies in *E. coli* reveal helical FtsZ at the center rather than a complete ring.^[7] Our model suggests a peak alignment around the bacterial diameter, though the curvature and twist may be far from the spontaneous values (Figures S13, S14). With adaptor proteins attaching the FtsZ filaments to the membrane in vivo, a similar behavior can be envisaged. The twist will be close to zero for radii around 0.5 μm, making it appear like a ring under normal fluorescence microscopy. Interestingly, 3D reconstructions from cryo-EM done on *C. crescentus* also show a helical arrangement rather than a closed ring.^[8] In the case when FtsZ would be generating an active constriction force, the alignment of the filament should be close to 90 degrees at all curvatures as the filaments would continuously strive to achieve the highest possible curvature. This is clearly not the case in our observations.

The ability of the FtsZ filament to align at such a range of radii in our experiments without assembling into its native conformation of helical structures suggests a substantial elasticity of the FtsZ filament. Most estimations of bending modulus are based on two dimensional analysis of filaments adsorbed on surfaces. We believe that this strongly affects the interpretations when surface interactions play a role. Our estimations of constrictive force from the model with curvature and twist yields a maximum force on the order of 0.06 pN (note that we assume that the standard deviations of the measured angles have a substantial contribution from thermal noise; Supporting Information, Text T1). If only spontaneous curvature was dominant, then the constrictive force would be around 3 pN. This is lower than the previously estimated values. With a highly flexible filament, models that rely mainly on FtsZ filament bending to generate constriction forces have to be reconsidered.

In summary, our experimental results indicate that FtsZ filaments have an intrinsic curvature and a spontaneous twist that allows them to assemble into a Z-ring at the equatorial region of the cell prior to division. Apart from nuclear occlusion and Min-protein oscillations as localization cues, minimization of the FtsZ polymer conformational energy by spontaneous curvature and twist may thus be an important additional cue, assembling and organizing the Z-ring as the platform for downstream processes of cytokinesis. Evolution of self-assembly in biological systems has led to generation of

several highly functional molecules performing specific functions, in this case, a polymer with an intrinsic helical structure. Filament-forming proteins are interesting from the point of understanding, as well as designing, self-assembling units. We believe that our approach of investigating the mechanics of curved polymers on curved membrane surfaces provides an attractive assay to quantitatively study mechanical forces, such as membrane curvature, and for protein recruitment and regulation in similar systems.

Received: June 4, 2012

Revised: July 5, 2012

Published online: August 31, 2012

Keywords: curvature · FtsZ · membranes · protein models · reconstitution

- [1] I. Hörger, E. Velasco, G. Rivas, M. Velez, P. Tarazona, *Biophys. J.* **2008**, *94*, L81.
- [2] A. Paez, P. Mateos-Gil, I. Horger, J. Mingorance, G. Rivas, M. Vicente, M. Velez, P. Tarazona, *PMC Biophys.* **2009**, *2*, 8.
- [3] S. S. Andrews, A. P. Arkin, *Biophys. J.* **2007**, *93*, 1872.
- [4] E. Fischer-Friedrich, B. M. Friedrich, N. S. Gov, *Phys. Biol.* **2012**, *9*, 016009.
- [5] W. Margolin, *Nat. Rev. Mol. Cell Biol.* **2005**, *6*, 862.
- [6] D. W. Adams, J. Errington, *Nat. Rev. Microbiol.* **2009**, *7*, 642.
- [7] G. Fu, T. Huang, J. Buss, C. Coltharp, Z. Hensel, J. Xiao, *PLoS One* **2010**, *5*, e12682.
- [8] Z. Li, M. J. Trimble, Y. V. Brun, G. J. Jensen, *EMBO J.* **2007**, *26*, 4694.
- [9] D. Popp, M. Iwasa, H. P. Erickson, A. Narita, Y. Maeda, R. C. Robinson, *J. Biol. Chem.* **2010**, *285*, 11281.
- [10] D. Popp, M. Iwasa, A. Narita, H. P. Erickson, Y. Maeda, *Biopolymers* **2009**, *91*, 340.
- [11] J. Mingorance, M. Tadros, M. Vicente, J. M. Gonzalez, G. Rivas, M. Velez, *J. Biol. Chem.* **2005**, *280*, 20909.
- [12] J. M. Gonzalez, M. Jimenez, M. Velez, J. Mingorance, J. M. Andreu, M. Vicente, G. Rivas, *J. Biol. Chem.* **2003**, *278*, 37664.
- [13] H. P. Erickson, *Proc. Natl. Acad. Sci. USA* **2009**, *106*, 9238.
- [14] Y. Chen, K. Bjornson, S. D. Redick, H. P. Erickson, *Biophys. J.* **2005**, *88*, 505.
- [15] S. Huecas, O. Llorca, J. Boskovic, J. Martin-Benito, J. M. Valpuesta, J. M. Andreu, *Biophys. J.* **2008**, *94*, 1796.
- [16] D. J. Turner, I. Portman, T. R. Dafforn, A. Rodger, D. I. Roper, C. J. Smith, M. S. Turner, *Biophys. J.* **2012**, *102*, 731.
- [17] M. Osawa, D. E. Anderson, H. P. Erickson, *EMBO J.* **2009**, *28*, 3476.
- [18] M. Osawa, D. E. Anderson, H. P. Erickson, *Science* **2008**, *320*, 792.
- [19] D. Bramhill, C. M. Thompson, *Proc. Natl. Acad. Sci. USA* **1994**, *91*, 5813.
- [20] H. P. Erickson, D. W. Taylor, K. A. Taylor, D. Bramhill, *Proc. Natl. Acad. Sci. USA* **1996**, *93*, 519.
- [21] J. Löwe, L. A. Amos, *EMBO J.* **1999**, *18*, 2364.
- [22] M. A. Oliva, S. Huecas, J. M. Palacios, J. Martin-Benito, J. M. Valpuesta, J. M. Andreu, *J. Biol. Chem.* **2003**, *278*, 33562.
- [23] X. C. Yu, W. Margolin, *EMBO J.* **1997**, *16*, 5455.
- [24] L. Hamon, D. Panda, P. Savarin, V. Joshi, J. Bernhard, E. Mucher, A. Mechulam, P. A. Curmi, D. Pastre, *Langmuir* **2009**, *25*, 3331.
- [25] H. P. Erickson, D. E. Anderson, M. Osawa, *Microbiol. Mol. Biol. Rev.* **2010**, *74*, 504.